Published in final edited form as:
J Mol Biol. 2008 February 22; 376(3): 645–657.

Identification and role of functionally important motifs in the 970 loop of *Escherichia coli* 16S ribosomal RNA

Ashesh A. Saraiya[1], **Tek N. Lamichhane**[2,3], **Christine S. Chow**[3], **John SantaLucia Jr.**[3], and **Philip R. Cunningham**[2,*]

2 *Department of Biological Sciences Wayne State University Detroit, MI. 48202, USA*

3 *Department of Chemistry Wayne State University Detroit, MI. 48202, USA*

Summary

The 970 loop (helix 31) of *Escherichia coli* 16S rRNA contains two modified nucleotides, m^2G966 and m^5C967. Positions A964, A969 and C970 are conserved among the Bacteria, Archaea and Eukarya. The nucleotides present at positions 965, 966, 967, 968 and 971, however, are only conserved and unique within each domain. All organisms contain a modified nucleoside at position 966, but the type of the modification is domain specific. Biochemical and structure studies have placed this loop near the P site and have shown it to be involved in the decoding process and in binding the antibiotic tetracycline. To identify the functional components of this rRNA hairpin, the eight nucleotides of the 970 loop of helix 31 were subjected to saturation mutagenesis and 107 unique functional mutants were isolated and analyzed. Non-random nucleotide distributions were observed at each mutated position among the functional isolates. Nucleotide identity at positions 966 and 969 significantly affects ribosome function. Ribosomes with single mutations of m^2G966 or m^5C967 produce more protein *in vivo* than wild-type ribosomes. Over-expression of initiation factor 3 (IF3) specifically restored wild-type levels of protein synthesis to the 966 and 967 mutants, suggesting that modification of these residues is important for IF3 binding and for the proper initiation of protein synthesis.

Keywords

Ribosome; rRNA; mutation; translation; modified nucleosides.

Introduction

Ribosomes are complexes of ribosomal proteins (rproteins) and ribosomal RNAs (rRNAs) that are responsible for the translation of messenger RNA into protein in all cells. It is well established that the rRNAs perform critical functional roles in each of the partial reactions of the translation process. Ribosomal RNAs contain several modified nucleosides that are clustered in regions of the rRNAs known to be functionally important.[1] Although their role in protein synthesis remains unclear, these modified nucleotides have been implicated in structural stability,[2, 3, 4] subunit assembly,[5] subunit association,[6] and in translational accuracy.[7, 8]

* *Corresponding author* E-mail address of the corresponding author: philc@wayne.edu.
[1]Current address: Department of Pharmaceutical Chemistry University of California, San Francisco 600 16th Street, Suite N572 San Francisco, CA. 94143−2280

In *Escherichia coli* 16S rRNA, the 970 hairpin consists of helix 31 (H31) and an eight-nucleotide loop (positions 964−971) containing modified nucleotides at positions 966 (2-methylguanosine, m^2G) and 967 (5-methylcytidine, m^5C) (Figure 1).[9] The size of the 970 loop is conserved within the Archaea, Bacteria and Eukarya, but nucleotide identity is conserved in all three domains only at positions A964, A969, and C970. Though a modified nucleoside is present at position 966 in all three domains, each domain is characterized by a specific modification.[10, 11] Bacterial 16S rRNAs contain m^2G at position 966, while the Eukarya and Archaea contain 1-methyl-3-(3-amino-3-carboxypropyl) pseudouridine[11], and 3-(3-amino-3-carboxypropyl) pseudouridine, respectively, at the corresponding position in their small-subunit rRNAs.[12, 13] The m^5C modification at position 967 is present only in Bacteria.

The importance of the 970 loop in ribosome function has been suggested by several biochemical, biophysical and genetic studies. Wilms *et al*. identified a UV photochemical cross-link between m^5C967 and C1400 in the P site of the decoding region that was disrupted in the presence of initiation factor 3 (IF3) [14, 15, 16]. Moazed and Noller showed that m^2G966 is protected from chemical probes by P-site-bound tRNA,[18] and Doring *et al*. identified a diazirine cross-link between m^2G966 and 2-thio C32 of the P-site-bound tRNA.[1, 17, 18]. Ribosome crystal structures also show a contact between the base of m^2G966 and the ribose of position 34 of the P-site-bound tRNA.[19, 20] These data suggest that the 970 loop is involved in the proper positioning of tRNA in the ribosomal P site. Jemiolo *et al*. found that single nucleotide substitutions at positions 966 and 967 did not affect the growth rate of *E. coli*, but that deletion of position 967 produced a dominant lethal phenotype when expressed from an inducible promoter in a multicopy plasmid.[21] Interestingly, Lesnyak et al. recently showed that disruption of the m^2G966 methyltransferase gene, *rsmD*, with a kanamycin resistance marker has little effect on the viability or growth rate of *E. coli* though the knockout strains were slightly less able to compete with wild-type cells when grown in rich medium.[22] Abdi and Fredrick, however, found that any mutation at position 966 resulted in a loss of ribosomal function (see Discussion).[23] Crystal structures of *Thermus thermophilus* 30S subunits[24] show interactions between the 970 loop and ribosomal proteins S9, S10, and S13. Residues m^2G966, m^5C967 and A968 make backbone contacts with protein S9[24], A964 and A969 make backbone contacts with protein S10[24], and U965, A969, and C970 make base contacts with protein S13[24]. In *E. coli*, however, S13 is truncated and does not interact with the 970 loop.[24, 25]

These studies suggest that the 970 loop plays an important role in protein synthesis. This notion is supported by structural studies showing that the 970 loop forms part of the primary binding site for tetracycline[26, 27] and by the isolation of a tetracycline-resistant strain of *Helicobacter pylori* that contains three mutations at positions 965, 966 and 967.[28] Here, we identify the sequence and structural motifs of the 970 loop nucleotides that are essential for ribosome function in bacteria and propose a model for the role of the 970 loop in protein synthesis.

Results

Identification of functionally important nucleotides and structural motifs

The 8 loop nucleotides, 964−971, of H31 were subjected to saturation mutagenesis using PCR and cloned in the specialized ribosome expression vector, pRNA123.[29, 30, 31] The plasmid pRNA123 contains the entire *rrnB* operon, the *lac* repressor ($lacI^q$), the CAT gene (*cam*), the GFP gene, and the ampicillin resistance gene (*bla*). The key features of this system are: 1) Transcription of the plasmid-encoded *rrnB* operon is regulated by the inducible *lacUV5* promoter; 2) the presence of $lacI^q$ insures an adequate supply of *lac* repressor protein to regulate rRNA transcription; 3) CAT and GFP transcription are constitutive, providing a constant supply of message; 4) the Shine-Dalgarno (SD) sequence of CAT and GFP have been changed from the wild-type, 5'-GGAGG, to 5'-AUCCC and the anti-Shine-Dalgarno (ASD) sequence of the plasmid-encoded 16S RNA gene has been changed from 5'-CCUCC to 5'-GGGAU; 5)

CAT and GFP mRNAs are not translated by chromosomally derived, wild-type ribosomes; 6) induction of the plasmid-encoded *rrnB* operon by IPTG renders cells resistant to chloramphenicol; 7) GFP production by the plasmid-encoded ribosomes allows high-throughput analysis of ribosome function in growing cultures.

E. coli DH5 cells were transformed with the pool of 970-loop mutants and functional mutants were selected on LB medium containing Amp (100 μg/ml), IPTG (1 mM), and chloramphenicol (100 μg/ml). A total of 107 chloramphenicol-resistant, functional 970 loop mutants were isolated, sequenced, assayed for ribosome function (Table 1) and analyzed to identify functionally important sequence and structural motifs.

Statistical analysis

To permit statistical analyses of the functional isolates, the selection strategy was designed to provide more variation in the mutant pool than is seen in nature.[30, 31] Nonrandom nucleotide distributions were observed at all positions in the selected pool (Table 2). Although all three possible mutations were isolated at each position, except position 964, preferences for specific nucleotides at each position were observed (Table 2). Position 964 shows a clear preference for adenosine, and guanosine was excluded. Guanosine was isolated in less than 10% of the active mutants at positions 965 and 968 ($p \leq 2.6 \times {}^{-9}$) and uridine was present in less than 10% of the mutants at positions 966, 967 and 971 ($p \leq 6.5 \times {}^{-6}$). A preference for purines over pyrimidines was observed at position 969 ($p = 1.3 \times 10^{-22}$) which is consistent with the participation of this residue in stacking interactions (discussed below) while adenosine and cytidine were preferred at position 970 ($p = 1.3 \times 10^{-20}$) suggesting that the ability of residues at this position to hydrogen bond using the Watson-Crick face is important for function (discussed below). These preferences are amplified when mutants with more than 20% function are analyzed (Table 2).

Overall, the pattern of nucleotide distribution among the functional mutants is similar to that observed when comparing phylogenetic variants (Table 2) with the exception of positions 965, 966, and 968. Pyrimidines were preferred at position 965 with cytidine present in 48 of the functional mutants and uridine, the wild-type nucleotide, present in 36 mutants. More purines than pyrimidines were isolated at position 966, which is consistent with the phylogenetic distribution, but more of the mutants had adenosine (46) than guanosine (40), the wild-type nucleotide, while at position 968 only 17 of the mutants contained the wild-type residue, adenosine, but 60 contained uridine.

Identifying nonrandom paired mutational patterns in sequence variants facilitates the identification of important constraints in RNA structures.[30, 31] To identify potential nucleotide interactions, we performed covariation analysis on all possible pairs of the mutated positions. Weak covariations between positions 964·965 ($p = 5.8 \times 10^{-5}$), 964·966 ($p = 7.3 \times 10^{-5}$), 964·967 ($p = 1.3 \times 10^{-2}$), 966·967 ($p = 4.7 \times 10^{-2}$), 966·969 ($p = 3.3 \times 10^{-2}$), 967·970 ($p = 1.2 \times 10^{-2}$), and 968·970 ($p = 1.7 \times 10^{-2}$) were observed (Figure 2). The two covariations involving positions 970 and 966, as well as the three covariations to position 964, suggest that these residues are involved in formation of functionally important structures.

Analysis of variance (ANOVA) was performed on the functional sequences to determine if a particular nucleotide present at any position among the mutants specifically affected ribosome function. Statistically significant ANOVAs were obtained at positions 966 ($p = 2.5 \times 10^{-4}$) and 969 ($p = 3.1 \times 10^{-2}$). These positions are part of two stacked base triples (Figure 2) in the 970 loop suggesting that these triples are important for ribosome function (discussed below).

Mutations at m^2G966 and m^5C967 produce hyperactive ribosomes

To examine the roles of the nucleotide modifications at positions 966 and 967 in H31, site-directed mutations were constructed at each position and analyzed to identify their effects on protein synthesis (Figure 3).

The m^2G966C mutation has little effect on ribosome function (96%); however, ribosomes containing the m^2G966A or the m^2G966U mutations produce more GFP than wild-type ribosomes (126% and 127%, respectively). Similarly, the m^5C967G mutation produces ribosomes with 107% activity, and the m^5C967A and m^5C967U mutant ribosome activities are 120% and 127% of wild-type ribosomes, respectively (Figure 3).

Modeling and UV cross-linking studies suggest that IF3 interacts with nucleotides in the 970 loop. Shapkina *et al.* showed that IF3 binding reduced the frequency of UV cross-links between $m^5C967 \times C1400$.[15] Using biochemical data from several studies, Pioletti *et al.* constructed a model of the IF3 N-terminus (IF3N) bound to the 30S subunit.[27] In their model, the N-terminal domain of IF3 (IF3N) is located in the P site and interacts with residues in the 970 loop.

Initiation of protein synthesis from the correct start codon is due to the interaction of the initiator tRNA, initiation factors and the P site of the 30S subunit. In particular, IF3 has been shown to play a significant role in start codon selection.[32, 33, 34] To examine the possibility that the hyperactive phenotype produced by mutations at 966 and 967 is due to an effect on IF3 binding, we cloned IF1, IF2 and IF3 into a pACYC177[35] derivative constructed in our lab, pKAN6, and placed them under control of the inducible *araBAD* promoter.[36, 37] As a negative control, we also measured the effect of initiation factor over-expression on GFP translation by ribosomes containing the G693U mutation in 16S rRNA. We previously showed that a single G693U mutation produced hyperactive ribosomes, similar to the phenotype observed with mutations at 966 and 967.[31] Each initiation factor was co-expressed with m^2G966U, m^5C967U or G693U. Over-expression of IF3 with U966 or U967 reduced GFP levels in the mutants to wild-type levels, but had no effect on GFP translation when co-expressed with U693 mutant ribosomes (Figure 4). Over-expression of IF1, however, did not restore the wild-type phenotype in any of the mutants tested. Over expression of IF2 was strongly inhibitory to even wild-type cells. These data are consistent with the existence of a specific functional interaction between the modified residues in the 970 loop and IF3.

Wilms *et al*. identified a UV cross-link between m^5C967 and C1400 in the ribosomal decoding region.[14] To determine if a functional interaction exists between positions m^5C967 and C1400, site-directed mutations between positions m^5C967 and 1400 were constructed and assayed (Table 3). In all of the 967/1400 mutants, ribosome function of the double mutants was approximately the product of each of the individual mutations suggesting that the effects of the mutations at each site are independent and that m^5C967 and C1400 do not interact during protein synthesis (Table 3), which is also consistent with X-ray structures of 30S and 70S ribosomes that have these residues greater than 6.5 Å apart.[19, 25, 38] Interestingly, the X-ray structures of *E. coli* and *T. thermophilus* 70S ribosomes show that O6 of G966 and N4 of C1400 are within hydrogen bonding distance, but not in the 30S subunit of *T. thermophilus*.[19, 25, 38] G966A mutant ribosomes are more active (126%) than wild type ribosomes, suggesting that this H-bond is important for wild-type function, since G966A is not capable of forming an isomorphous H-bond with C1400. Mutation of C1400 to an A or G resulted in 17% and 16% function, respectively. The *in vivo* activity of ribosomes containing the C1400U mutation, however, is 130% compared to wild-type ribosomes. The hyperactive C1400U mutant was not complemented by over-expression of IF3 (Figure 4). These data suggest that hyperactivity in the m^5C967 mutants is not due to interference with possible C1400 interactions and that hyperactivity due to mutations at 1400 is probably caused by a different mechanism than that observed in the 970 loop mutants (discussed below).

Discussion

The eight-nucleotide sequence of the 970 loop of helix 31 is conserved within each of the three phylogenetic domains but only A964, A969, and C970 are conserved throughout all three domains. The 970 loop also contains two of the eleven modified nucleosides in *E. coli* 16S rRNA, m^2G966 and m^5C967. To examine the role of H31 in protein synthesis and identify functionally important nucleotides, sequence motifs, and structural motifs in the 970 loop, we randomly mutated all eight of the conserved loop nucleotides (964−971) and selected, sequenced and assayed viable mutants.

971 anchors the 970 loop

In the 30S crystal structure[38], 971 is flipped out and binds into a pocket formed by the backbones of nucleotides at positions 949, 950, 1363, 1364, and 1365 of 16S rRNA. The wild type, G971, forms three hydrogen bonds within this pocket. Uridine is underrepresented at position 971, among the functional mutants (Table 2). The ribosome is known to undergo conformational changes during translation.[39, 40, 41, 42] Specifically, the head portion of the 30S subunit moves ~10 Å during translocation to open and close the mRNA channel.[40 39, 43] Flexibility in the 970 loop during movement of the head may allow it to block access of P-site tRNA, f-met tRNA, or IF3 to the P site. Hydrogen bonding at the exposed nucleotide, 971, may serve to limit the mobility of the 970 loop and to connect the movement of the 970 loop to the movement of the ribosome during protein synthesis. The reduced hydrogen bonding and stacking ability of the G971U mutant may increase the mobility of the 970 loop which may in turn interfere with the binding of P-site tRNA as well as IF3 to the 30S subunit.

Importance of the 966, 967, and 968 stack

An active role for the loop nucleotides of H31 in protein synthesis has been implicated by a number of different studies. Position 966 of the 970 loop is protected from chemical modification by the P-site tRNA[17, 44] and cross-linked to P-site tRNA[45] and position 967 has been UV cross-linked to position 1400 which is a component of the P site.[14] As previously noted, modeling studies with IF3 fragments also suggest that IF3 interacts with positions 966:967:968. [27]

Aduri et al. constructed a model of the *E. coli* 30S ribosome with all of the modifications present.[46] The results show that the methyl groups in m^2G966 and m^5C967 extend their stacking surface areas. The extended surface contact stabilizes the rather unusual 970 loop structure, which has few intra-loop H-bond interactions. In addition, the methyl group of m^2G966 is within van der Waals contact of Arg128 of protein S9 in the *T. thermophilus* 30S structure with m^2G966 modeled in, suggesting that m^2G966 stabilizes S9 binding through hydrophobic interactions.[19, 24, 46]

The base of 966 interacts with the backbone of the P-site tRNA at position 34[20] and in the saturation mutagenesis showed a preference for purines. We found that among the functional mutants, adenosine was present more often than m^2G at position 966. It is possible that adenosine was preferred because it lacks a functional group at the N2 position and therefore allowed more variation in the other mutated nucleotides of the loop without interfering with the binding of tRNA or other ligands at the P site.

There is no indication that m^5C967 and A968 directly interact with P-site tRNA, but they do position m^2G966 so that it can interact with P-site tRNA. [19, 20] Proper positioning of the nucleotide at position 966 is therefore one of the factors constraining mutations at positions 967 and 968 among the functional mutants. Of the 107 functional isolates, 42 contained the wild-type C at position 967. Of the remaining 65 mutants, 55 contained a purine at this position.

In the absence of the m^5C967 modification, the presence of a purine would allow for greater stabilization of the stack. Interestingly, of the 55 clones containing a purine at position 967, 41 contained an A while only 14 contained a G. Thus, 83 clones contained either an A or C at position 967 suggesting an additional preference for a hydrogen bond donor at position N4 or N6. Finally, the wild-type A968 was underrepresented in favor of A968U among the selected mutants. This may be a consequence of the preference for N4 or N6 at position 967 because the presence of an O4 in the A968U mutant would create the potential for additional dipole interactions between the O4 and the N4 or N6 of 967, increasing the stability of the 967, 969, 970 stack.

Site-directed mutations at positions m^2G966 and m^5C967 resulted in higher levels of function when compared to the wild-type sequence (Figure 3). These data differ from those of Abdi and Fredrick who found that m^2G966 mutations reduced protein synthesis to 10−30% of wild-type levels.[23] These investigators used a derivative of our specialized system.[29, 30] The primary differences between the systems are that the reporter is *lacZ* (containing the modified SD sequence), which is incorporated in the chromosome in a recombinant lambda prophage, and that the plasmid expresses only the 16S rRNA gene (with the modified ASD) but not the remainder of the *rrnB* operon. Thus, it is possible that expression of the 16S rRNA gene in this construct creates an imbalance in the ratio between 30S and 50S subunits and/or that the 16S rRNA is incorrectly processed in the absence of the entire *rrnB* transcript[47] resulting in decreased translation of the reporter mRNA. This effect may have been amplified in the m^2G966 mutants due to their potential effect on initiation. Alternatively, it is possible that a difference in the reporter constructs somehow differentially affects translation by mutant ribosomes. A similar discrepancy occurs regarding mutations at position 1400. Our findings indicate that mutation of C1400 to an A or G resulted in 17% and 16% function, respectively, and that ribosomes containing the C1400U mutation, produced 30% more GFP than the wild-type ribosomes. Abdi and Fredrick found ribosomes expressing C1400 to A or G produced approximately 5% and 9% as much β-galactosidase as wild-type ribosomes, respectively, and that C1400U-containing ribosomes were approximately 50% as active as wild-type ribosomes[23] Hui *et al.*, using a specialized ribosome system with a different SD-ASD combination and with human growth hormone (hGH) as the reporter, found that A1400 and G1400 mutations produced ribosomes that were 50% and 20% as active as wild-type ribosomes and that the U1400 mutation had no effect (100%) on the amount of hGH produced.[48] *In vitro* analyses of reconstituted ribosomes containing single mutations at position 1400 revealed little effect on subunit association and P-site-tRNA binding, but the mutants showed a significant increase in poly(Phe-Val) synthesis.[49] In addition, tRNA binding at the A site for the A1400 and G1400 mutants was 80% and 60% of the wild type, but 130% of the wild type in the U1400 mutant.

The higher function we observed for the m^2G966 and m^5C967 mutations when compared to the wild type, indicates that the mutations cause an increase in the rate of protein synthesis.[50] The most likely explanation for this result is that the mutations have a direct effect on the interaction between the 970 loop and tRNA in the ribosomal P-site.[19, 20] An alternative explanation is that the mutations affect factor binding. *In vitro* translation experiments with mutant initiator tRNA anticodon fragments and IF3 suggest that IF3 discriminates initiator tRNA from aminoacyl-tRNA during initiation.[51] Disruption of IF3 binding may therefore interfere with the discrimination of initiator tRNA, leading to a decrease in the stringency for initiator tRNA selection and an increased rate of initiation. If IF3-binding were affected by mutations at m^2G966 and m^5C967, it seemed possible that over-expression of IF3 might specifically complement mutations at these positions. To test this hypothesis, we over-expressed all three initiation factors in the presence of m^2G966U and m^5C967U to see if wild-type levels of function would be restored.

Over-expression of IF3, but not IF1 and IF2, with 30S subunits containing mutations at position 966 or 967, restores wild-type levels of GFP synthesis but does not affect GFP synthesis in strains co-expressing mutations at other loci in 16S rRNA that also increase GFP production (Figure 4).[31] These data indicate that mutations at positions 966 or 967 interfere with IF3 binding and that this defect can be alleviated by increased production of IF3.

Importance of the 965, 969, and 970 stack

In ribosome crystal structures, U965, A969, and C970 form a second three-base stack.[24, 25, 38] The universal conservation of U969 and C970, suggests that the formation of this stack is an important determinant of ribosome function. Position 964 is an adenosine in the wild-type 970 sequence (Figure 1) and is the most conserved residue among the 970 loop functional mutants. Only 15 mutations were isolated at this position and guanosine was excluded (Table 2). These data suggest that a sterically bulky polar group at the C2 position inhibits ribosome function. Exclusion of G at position 964 may be due to disruption of the 965:969:970 stack. In modeling studies in which guanine was substituted for A964, the N2 of guanine sterically clashes with the sugar of position 970 which in-turn may disrupt the 965:969:970 stack (Figure 5). A similar observation was made at position 697 in 16S rRNA in a previous study.[31]

A statistically significant nucleotide covariation was observed between positions 964 and 965 (Figure 2). None of the 15 pyrimidine mutations isolated at position 964 also contained one of the 39 U965 or G965 mutations identified in the selected pool suggesting that co-existence of these mutations inhibits ribosome function. These data indicate that the 965:969:970 stack is essential for ribosome function and that the presence of only 15 mutations at position 964, all of which are pyrimidines, is because most of the 964 mutations present in the pool prior to selection were eliminated in the functional pool because they disrupted the 965:969:970 stack.

The X-ray crystallographic studies of the *E. coli* 70S ribosome performed by Schuwirth *et al.* revealed two different 70S structures.[25] The ribosome head in structure 2 is rotated around the neck 6° toward the E site in comparison to structure 1, while the head in structure 1 is rotated around the neck 6° toward the E site in comparison to the 5.5 Å 70S *Thermus* structure.[20] This represents a total rotation of ~ 12° (20 Å) between structure 2 and the 5.5 Å 70S *Thermus* structure.[20] This rotation around the neck may represent a mechanism for translocation. The 970 loop of the Ogle 30S structure[39] and the Schuwirth structure 2 are similar. The Schuwirth structure 1, however, is different. Position 969 is in the same orientation as in the Schuwirth structure 2 and the Ogle structure; however, positions 965 and 970 of the 965:969:970 stack are perpendicular to position 969 rather than stacked. This change in the 965:969:970 stack may represent a disruption in the IF3 binding site to inhibit binding of IF3N to the 965:969:970 stack in the absence of f-met tRNA in the P site.

Role of the 970 loop in IF3 binding

Our data show that mutations at 966 and 967 produce hyperactive ribosomes and that this phenotype is specifically complemented by overexpression of IF3. Complementation by IF3 indicates that the 966 and 967 mutations decrease the affinity of IF3 for the 30S subunit. This effect may be the result of a direct interaction of IF3 with the 970 loop or the result of an indirect effect of a conformational change that affects another IF3 binding site.[19, 52, 53, 54, 55] Chemical footprinting[52] and crosslinking[15] do not support a direct interaction between the 970 loop and IF3. McCutcheon et al., however, showed that binding of IF3 results in a conformational change in the 30S subunit.[56] This is consistent with an indirect effect of 970 loop mutations on IF3 binding. The N terminus of IF3 is connected to the C terminus by a 14 amino acid alpha helix that allows the N terminus of IF3 to move.[57] X-ray crystallographic studies[27] show that the IF3 C-domain interacts with the 690 and 790 loops in 16S rRNA, consistent with the hydroxyl radical footprinting studies.[52] Although IF3N by itself does not

bind to the 30S subunit, its presence is required for wild-type binding kinetics of IF3 and its main role appears to be stabilization of the IF3−30S complex..[55] Attempts to obtain crystal structures of the 30S ribosome complexed with the IF3 N-domain, however were unsuccessful.[27] Pioletti et al. therefore used molecular modeling of the NMR and X-ray structures of isolated IF3 to dock the IF3 N-domain.[27] The modeling studies place IF3N in proximity to the P-site with possible interactions with H28, H29, H31, H34 and H44. The 970 loop interactions (H31) involved the 966−68 stack. Direct interactions between IF3 and the 970 loop, however, have not been reported in other studies. Thus, it may be that the 970 loop either directly or indirectly forms a transient binding site for IF3N.

The functional importance of the 970 loop and the fact that it contains domain-specific modifications provide a unique opportunity for its use as a drug target for the development of new anti-infectives. The studies presented here identify structural and sequence motifs of the 970 loop that are essential for proper ribosome function and will facilitate targeting new anti-infectives to these critical motifs.[58]

Materials and Methods

Reagents

Restriction enzymes, ligase, and calf intestine alkaline phosphatase were from New England Biolabs and from Gibco-BRL. Sequencing modified DNA polymerase, nucleotides, and sequencing buffers were from Epicentre Technologies. Oligonucleotides were either purchased from Midland Certified Reagent Company (Midland, TX.) or IDT DNA (Coralville, IA). AmpliTaq DNA polymerase and PCR reagents were from Perkin-Elmer-Cetus (Boston, MA).

Plasmids and mutagenesis

The plasmid pRNA123 contains the *E. coli rrnB* operon, with the 16S rRNA containing an altered anti-Shine-Dalgarno (ASD) sequence, under transcriptional control of a *lacUV5* promoter. The plasmid also contains the chloramphenicol acetyltransferase (CAT) and green fluorescent protein (GFP) reporter genes with Shine-Dalgarno (SD) sequences complementary to the ASD sequence of the plasmid 16S rRNA [29, 59, 60, 61]. Therefore, the CAT and GFP mRNAs are specifically translated only by ribosomes containing the plasmid-encoded 30S subunits. In addition, ribosomes containing plasmid-encoded 30S subunits do not translate normal host mRNAs. Thus, mutations in plasmid-encoded ribosomes only affect the translation of CAT and GFP mRNAs without affecting the translation of other cellular mRNAs. The CAT and GFP dual reporter system provides an efficient and high throughput system for directly selecting and analyzing 16S rRNA the effect of mutations that affect protein synthesis.

All 970 loop mutations were constructed using recombinant PCR.[62, 63, 64] PCR 1 was performed with primers 970 loop mut (5'- GGA TGT CAA GAC CAG GTA AGG TTC TTC GNN NNN NNN CGA ATT AAA CCA CAT GCT CCA CCG -3') and 16S *Avr*II (5'-ACG TCG CAA GAC CAA AGA GG -3') and PCR 2 was performed with primers 970 loop R (5'-CCT GGT CTT GAC ATC CAC GG -3') and 16S *Xba*I (5'- GGT CGG CGA CTT TCA CTC AC -3'). The resulting PCR products were used as templates for PCR 3 along with the outside primers to amplify the full insert.

Construction of mutations—All mutations were constructed in a modified version of pRNA123 containing a mutation at the 970 loop (964-UCCCCCGU −971) that renders the 30S subunit inactive. Random mutations were introduced in the 16S rRNA gene of pRNA123 by replacing the wild-type sequence between the *Bgl*II and *BstE*II cut sites with a fragment containing PCR directed random mutations.

Selection of functional mutants—Transformants were incubated at 37° C with shaking in SOC medium for one hour to allow for the expression of the Amp^R gene. A sample of the culture was plated on LB+Amp100 plates to determine the transformation efficiency. A total of 37 transformants were randomly chosen, sequenced and the nucleotide distribution analyzed (not shown). Nucleotide distribution at each of the mutated positions in the mutant pool was random prior to chloramphenicol selection. IPTG (isopropyl-β-D-thiogalactopyranoside) was then added to the remaining culture to a concentration of 1mM and incubated at 37° C with shaking for an additional three hours to induce rRNA synthesis. The culture was then plated on LB+Amp100+IPTG agar with 100 μg/ml chloramphenicol. Chloramphenicol resistant survivors (approximately 10%) were selected, sequenced and assayed. A total of 10,000 mutants were screened.

Construction of single mutants in 16S rRNA—Single mutants were constructed in pRNA272, a derivative of pRNA123[29, 30] containing a unique *Apa*I site in the 16S rRNA gene. Single mutants at positions 966 and 967 were made using site-directed PCR (16S C967D (5'- AAT GAA TTG ACG GGG GCC CGC ACA AGC GGT GGA GCA TGT GGT TTA ATT CGA TGD AAC GCG AAG AAC CTT A -3') or 16S G966H (5'- AAT GAA TTG ACG GGG GCC CGC ACA AGC GGT GGA GCA TGT GGT TTA ATT CGA THC AAC GCG AAG AAC CTT A -3') with 16S *Xba*I) and cloned into pRNA272 using *Apa*I and *Rsr*II restriction enzymes. Mutations at position 1400 were made using site-directed PCR (16S C1400D (5' GTT CCC GGG CCT TGT ACA CAC DGC CCG TCA CAC CAT G 3') and 23S 750R (5'- GGT TCG GTC CTC CAG TTA GT -3')) and cloned into pRNA272 using *Xba*I and *Bsr*GI restriction enzymes. Each mutant was sequenced to confirm the presence of the mutation and assayed for function using GFP assays.

Construction of double mutants in 16S rRNA—Double mutants were constructed from single mutant constructs in pRNA272. Both the 1400 and 967 single mutants were digested with *Rsr*II and *Xho*I. Fragments containing the single mutations were ligated together to form the double mutants. These clones were then transformed into *E. coli* DH5 cells. Each mutant was sequenced to confirm the presence of the mutation and assayed for function using GFP assays.

Bacterial strains and media

All plasmids were maintained and expressed in *E. coli* DH5 (*supE44, hsdR17, recA1, endA1, gyrA96, thi-1, relA1*).[65] Cultures were maintained in LB medium[66] or LB medium containing 100 μg/ml ampicillin (LB+Ap100). To induce synthesis of plasmid-derived rRNA from the *lacUV5* promoter; IPTG (isopropyl-beta-D-thiogalactopyranoside) was added to a final concentration of 1 mM at the times indicated in each experiment. Strains were transformed by electroporation[67] using a Gibco-BRL Cell Porator. Unless otherwise indicated, transformants were grown in SOC medium[65] for one hour prior to plating on selective medium to allow expression of plasmid-derived genes.

Green fluorescent protein (GFP) assay

Overnight cell cultures were grown in LB+Ap100 then diluted 1:100, induced in LB+Amp100 + IPTG (1 mM) medium, and grown at 37 °C with shaking for 24 hours. To measure GFP, 0.5 mL of each culture was pelleted and washed twice with 0.5 mL of HN buffer (20 mM HEPES pH 7.4 and 0.85% NaCl) and resuspended in 0.5 mL of HN buffer. 100 μL of washed cell suspension was transferred to a 96 well clear bottom microtiter plate for analysis. Cell density (λ = 600 nm) was measured using a SPECTRAmax 190 (Molecular Devices, Sunnyvale, CA) and GFP fluorescence (excitation = 395 nm and emission = 509 nm) was measured using a SPECTRAmax GEMINI (Molecular Devices, Sunnyvale, CA). For each culture, fluorescence

was divided by A_{600} and presented as a percentage of the wild type. Values represent the average of at least three assays on three separate cultures done on different days.

Over-expression of initiation factors

The genes encoding *E. coli* IF1, IF2, and IF3 were cloned into pKAN6, a derivative of pACYC177[35], under the control of P_{BAD}.[36] pKAN6 containing an IF was co-transformed into *E. coli* DH5 with pRNA123 harboring either the m^2G966U, m^5C967U, C1400U, G693U mutations or wild-type 16S rRNA and grown on LB+Amp100+Kan50 plates. Clones containing both plasmids were grown overnight at 37° C with shaking in LB+Amp100+Kan50. The culture was diluted 1:100 in LB+Amp100+Kan50 and induced with IPTG (1 mM) and L-Arabinose (0.2%). The induced cultures were grown for 24 hours at 37° C with shaking and assayed for GFP function as described above.

ACKNOWLEDGEMENTS

We thank Kris Ann Baker and Laurie Ann Boore for helpful discussions and editing of this manuscript. We also thank Pirro Saro for contributing the modified nucleoside functionalities in RNA-1−2−3. This work was supported by National Institutes of Health under grant U01AI061192.

References

1. Brimacombe R, Mitchell P, Osswald M, Stade K, Bochkariov D. Clustering of modified nucleotides at the functional center of bacterial ribosomal RNA. FASEB J 1993;7:161–7. [PubMed: 8422963]
2. Meroueh M, Grohar PJ, Qiu J, SantaLucia J, Jr. Scaringe SA, Chow CS. Unique structural and stabilizing roles for the individual pseudouridine residues in the 1920 region of *Escherichia coli* 23S rRNA. Nucleic Acids Res 2000;28:2075–83. [PubMed: 10773075]
3. Rife JP, Cheng CS, Moore PB, Strobel SA. N 2-methylguanosine is iso-energetic with guanosine in RNA duplexes and GNRA tetraloops. Nucleic Acids Res 1998;26:3640–4. [PubMed: 9685477]
4. Heus HA, Van Kimmenade JM, van Knippenberg PH, Hinz HJ. Calorimetric measurements of the destabilisation of a ribosomal RNA hairpin by dimethylation of two adjacent adenosines. Nucleic Acids Res 1983;11:203–10. [PubMed: 6346264]
5. Cunningham PR, Richard RB, Weitzmann CJ, Nurse K, Ofengand J. The absence of modified nucleotides affects both *in vitro* assembly and *in vitro* function of the 30S ribosomal subunit of *Escherichia coli*. Biochimie 1991;73:789–96. [PubMed: 1764523]
6. Lee K, Holland-Staley CA, Cunningham PR. Genetic approaches to studying protein synthesis: effects of mutations at Psi516 and A535 in *Escherichia coli* 16S rRNA. J. Nutr 2001;131:2994S–3004S. [PubMed: 11694635]
7. van Buul CP, Visser W, van Knippenberg PH. Increased translational fidelity caused by the antibiotic kasugamycin and ribosomal ambiguity in mutants harbouring the ksgA gene. FEBS Lett 1984;177:119–24. [PubMed: 6568181]
8. Widerak M, Kern R, Malki A, Richarme G. U2552 methylation at the ribosomal A-site is a negative modulator of translational accuracy. Gene 2005;347:109–14. [PubMed: 15715963]
9. Cannone JJ, Subramanian S, Schnare MN, Collett JR, D'Souza LM, Du Y, Feng B, Lin N, Madabusi LV, uuml, ller KM, Pande N, Shang Z, Yu N, Gutell RR. The Comparative RNA Web (CRW) Site: an online database of comparative sequence and structure information for ribosomal, intron, and other RNAs. BMC Bioinformatics 2002;3:2. [PubMed: 11869452]
10. Kowalak JA, Bruenger E, Crain PF, McCloskey JA. Identities and phylogenetic comparisons of posttranscriptional modifications in 16 S ribosomal RNA from *Haloferax volcanii*. J. Biol. Chem 2000;275:24484–9. [PubMed: 10818097]
11. Maden BE. The numerous modified nucleotides in eukaryotic ribosomal RNA. Prog. Nucleic Acid Res. Mol. Biol 1990;39:241–303. [PubMed: 2247610]
12. Balch WE, Fox GE, Magrum LJ, Woese CR, Wolfe RS. Methanogens: reevaluation of a unique biological group. Microbiol. Rev 1979;43:260–96. [PubMed: 390357]

13. Woese CR, Gupta R, Hahn CM, Zillig W, Tu J. The phylogenetic relationships of three sulfur dependent archaebacteria. Syst. App.l Microbiol 1984;5:97–105.

14. Wilms C, Noah JW, Zhong D, Wollenzien P. Exact determination of UV-induced crosslinks in 16S ribosomal RNA in 30S ribosomal subunits. RNA 1997;3:602–12. [PubMed: 9174095]

15. Shapkina TG, Dolan MA, Babin P, Wollenzien P. Initiation factor 3-induced structural changes in the 30 S ribosomal subunit and in complexes containing tRNA(f)(Met) and mRNA. J. Mol. Biol 2000;299:615–28. [PubMed: 10835272]

16. Ofengand J, Gornicki P, Chakraburtty K, Nurse K. Functional conservation near the 3' end of eukaryotic small subunit RNA: photochemical crosslinking of P site-bound acetylvalyl-tRNA to 18S RNA of yeast ribosomes. Proc .Natl. Acad. Sci. USA 1982;79:2817–21. [PubMed: 7045872]

17. Moazed D, Noller HF. Binding of tRNA to the ribosomal A and P sites protects two distinct sets of nucleotides in 16 S rRNA. J. Mol. Biol 1990;211:135–45. [PubMed: 2405162]

18. von Ahsen U, Noller HF. Identification of bases in 16S rRNA essential for tRNA binding at the 30S ribosomal P site. Science 1995;267:234–7. [PubMed: 7528943]

19. Selmer M, Dunham CM, Murphy F. V. t. Weixlbaumer A, Petry S, Kelley AC, Weir JR, Ramakrishnan V. Structure of the 70S ribosome complexed with mRNA and tRNA. Science 2006;313:1935–42. [PubMed: 16959973]

20. Yusupov MM, Yusupova GZ, Baucom A, Lieberman K, Earnest TN, Cate JH, Noller HF. Crystal structure of the ribosome at 5.5 A resolution. Science 2001;292:883–96. [PubMed: 11283358]

21. Jemiolo DK, Taurence JS, Giese S. Mutations in 16S rRNA in *Escherichia coli* at methyl-modified sites: G966, C967, and G1207. Nucleic Acids Res 1991;19:4259–65. [PubMed: 1714565]

22. Lesnyak DV, Osipiuk J, Skarina T, Sergiev PV, Bogdanov AA, Edwards A, Savchenko A, Joachimiak A, Dontsova OA. Methyltransferase that modifies guanine 966 of the 16 S rRNA: functional identification and tertiary structure. J. Biol. Chem 2007;282:5880–7. [PubMed: 17189261]

23. Abdi NM, Fredrick K. Contribution of 16S rRNA nucleotides forming the 30S subunit A and P sites to translation in *Escherichia coli*. RNA 2005;11:1624–32. [PubMed: 16177132]

24. Brodersen DE, Clemons WM, Jr. Carter AP, Wimberly BT, Ramakrishnan V. Crystal structure of the 30 S ribosomal subunit from Thermus thermophilus: structure of the proteins and their interactions with 16 S RNA. J. Mol. Biol 2002;316:725–68. [PubMed: 11866529]

25. Schuwirth BS, Borovinskaya MA, Hau CW, Zhang W, Vila-Sanjurjo A, Holton JM, Cate JH. Structures of the bacterial ribosome at 3.5 A resolution. Science 2005;310:827–34. [PubMed: 16272117]

26. Brodersen DE, Clemons WM, Jr. Carter AP, Morgan-Warren RJ, Wimberly BT, Ramakrishnan V. The structural basis for the action of the antibiotics tetracycline, pactamycin, and hygromycin B on the 30S ribosomal subunit. Cell 2000;103:1143–54. [PubMed: 11163189]

27. Pioletti M, Schlunzen F, Harms J, Zarivach R, Gluhmann M, Avila H, Bashan A, Bartels H, Auerbach T, Jacobi C, Hartsch T, Yonath A, Franceschi F. Crystal structures of complexes of the small ribosomal subunit with tetracycline, edeine and IF3. EMBO J 2001;20:1829–39. [PubMed: 11296217]

28. Dailidiene D, Bertoli MT, Miciuleviciene J, Mukhopadhyay AK, Dailide G, Pascasio MA, Kupcinskas L, Berg DE. Emergence of tetracycline resistance in Helicobacter pylori: multiple mutational changes in 16S ribosomal DNA and other genetic loci. Antimicrob Agents Chemother 2002;46:3940–6. [PubMed: 12435699]

29. Lee K, Holland-Staley CA, Cunningham PR. Genetic analysis of the Shine-Dalgarno interaction: selection of alternative functional mRNA-rRNA combinations. RNA 1996;2:1270–85. [PubMed: 8972775]

30. Lee K, Varma S, SantaLucia J, Jr. Cunningham PR. *In vivo* determination of RNA structure-function relationships: analysis of the 790 loop in ribosomal RNA. J. Mol. Biol 1997;269:732–43. [PubMed: 9223637]

31. Morosyuk SV, SantaLucia J, Jr. Cunningham PR. Structure and function of the conserved 690 hairpin in *Escherichia coli* 16 S ribosomal RNA. III. Functional analysis of the 690 loop. J. Mol. Biol 2001;307:213–28. [PubMed: 11243815]

32. Sussman JK, Simons EL, Simons RW. *Escherichia coli* translation initiation factor 3 discriminates the initiation codon *in vivo*. Mol Microbiol 1996;21:347–60. [PubMed: 8858589]

33. O'Connor M, Gregory ST, Rajbhandary UL, Dahlberg AE. Altered discrimination of start codons and initiator tRNAs by mutant initiation factor 3. RNA 2001;7:969–78. [PubMed: 11453069]
34. Tedin K, Moll I, Grill S, Resch A, Graschopf A, Gualerzi CO, Blasi U. Translation initiation factor 3 antagonizes authentic start codon selection on leaderless mRNAs. Mol Microbiol 1999;31:67–77. [PubMed: 9987111]
35. Chang AC, Cohen SN. Construction and characterization of amplifiable multicopy DNA cloning vehicles derived from the P15A cryptic miniplasmid. J Bacteriol 1978;134:1141–56. [PubMed: 149110]
36. Greenfield L, Boone T, Wilcox G. DNA sequence of the *araBAD* promoter in *Escherichia coli* B/r. Proc .Natl. Acad. Sci. USA 1978;75:4724–8. [PubMed: 368797]
37. Kaplan DA, Greenfield L, Boone T, Wilcox G. Hybrid plasmids containing the *araBAD* genes of *Escherichia coli* B/r. Gene 1978;3:177–89. [PubMed: 357248]
38. Wimberly BT, Brodersen DE, Clemons WM, Jr. Morgan-Warren RJ, Carter AP, Vonrhein C, Hartsch T, Ramakrishnan V. Structure of the 30S ribosomal subunit. Nature 2000;407:327–39. [PubMed: 11014182]
39. Ogle JM, Murphy FV, Tarry MJ, Ramakrishnan V. Selection of tRNA by the ribosome requires a transition from an open to a closed form. Cell 2002;111:721–32. [PubMed: 12464183]
40. Frank J, Agrawal RK. A ratchet-like inter-subunit reorganization of the ribosome during translocation. Nature 2000;406:318–22. [PubMed: 10917535]
41. VanLoock MS, Agrawal RK, Gabashvili IS, Qi L, Frank J, Harvey SC. Movement of the decoding region of the 16 S ribosomal RNA accompanies tRNA translocation. J. Mol. Biol 2000;304:507–15. [PubMed: 11099376]
42. Valle M, Zavialov A, Sengupta J, Rawat U, Ehrenberg M, Frank J. Locking and unlocking of ribosomal motions. Cell 2003;114:123–34. [PubMed: 12859903]
43. Schluenzen F, Tocilj A, Zarivach R, Harms J, Gluehmann M, Janell D, Bashan A, Bartels H, Agmon I, Franceschi F, Yonath A. Structure of functionally activated small ribosomal subunit at 3.3 angstroms resolution. Cell 2000;102:615–23. [PubMed: 11007480]
44. Moazed D, Noller HF. Transfer RNA shields specific nucleotides in 16S ribosomal RNA from attack by chemical probes. Cell 1986;47:985–94. [PubMed: 2430725]
45. Doring T, Mitchell P, Osswald M, Bochkariov D, Brimacombe R. The decoding region of 16S RNA; a cross-linking study of the ribosomal A, P and E sites using tRNA derivatized at position 32 in the anticodon loop. EMBO J 1994;13:2677–85. [PubMed: 7516877]
46. Aduri R, Psciuk BT, Saro P, Taniga H, Schlegel HB, SantaLucia J. AMBER Force Field Parameters for the Naturally Occurring Modified Nucleosides in RNA. J. Chem. Theory Comput 2007;3:1464–1475.
47. Srivastava AK, Schlessinger D. Mechanism and regulation of bacterial ribosomal RNA processing. Annu Rev Microbiol 1990;44:105–29. [PubMed: 1701293]
48. Hui AS, Eaton DH, de Boer HA. Mutagenesis at the mRNA decoding site in the 16S ribosomal RNA using the specialized ribosome system in *Escherichia coli*. EMBO J 1988;7:4383–8. [PubMed: 2468489]
49. Cunningham, PR.; Weitzmann, C.; Nègre, D.; Sinning, JG.; Frick, V.; Nurse, K.; Ofengand, J. In vitro analysis of the role of rRNA in protein synthesis: Site-specific mutation and methylation.. In: Hill, W.; Dahlberg, AE.; Garrett, R.; Moore, P.; Schlessinger, D.; Warner, J., editors. The Ribosome. Structure, Function and Evolution. ASM Press; Washington DC: 1990.
50. Laursen BS, Sorensen HP, Mortensen KK, Sperling-Petersen HU. Initiation of protein synthesis in bacteria. Microbiol Mol Biol Rev 2005;69:101–23. [PubMed: 15755955]
51. Hartz D, Binkley J, Hollingsworth T, Gold L. Domains of initiator tRNA and initiation codon crucial for initiator tRNA selection by *Escherichia coli* IF3. Genes Dev 1990;4:1790–800. [PubMed: 1701151]
52. Dallas A, Noller HF. Interaction of translation initiation factor 3 with the 30S ribosomal subunit. Mol. Cell 2001;8:855–64. [PubMed: 11684020]
53. Fabbretti A, Pon CL, Hennelly SP, Hill WE, Lodmell JS, Gualerzi CO. The real-time path of translation factor IF3 onto and off the ribosome. Mol. Cell 2007;25:285–96. [PubMed: 17244535]

54. Lomakin IB, Shirokikh NE, Yusupov MM, Hellen CU, Pestova TV. The fidelity of translation initiation: reciprocal activities of eIF1, IF3 and YciH. EMBO J 2006;25:196–210. [PubMed: 16362046]
55. Petrelli D, LaTeana A, Garofalo C, Spurio R, Pon CL, Gualerzi CO. Translation initiation factor IF3: two domains, five functions, one mechanism? EMBO J 2001;20:4560–9. [PubMed: 11500382]
56. McCutcheon JP, Agrawal RK, Philips SM, Grassucci RA, Gerchman SE, Clemons WM, Jr. Ramakrishnan V, Frank J. Location of translational initiation factor IF3 on the small ribosomal subunit. Proc .Natl. Acad. Sci. USA 1999;96:4301–6. [PubMed: 10200257]
57. Biou V, Shu F, Ramakrishnan V. X-ray crystallography shows that translational initiation factor IF3 consists of two compact alpha/beta domains linked by an alpha-helix. EMBO J 1995;14:4056–64. [PubMed: 7664745]
58. Laios E, Waddington M, Saraiya AA, Baker KA, O'Connor E, Pamarathy D, Cunningham PR. Combinatorial genetic technology for the development of new anti-infectives. Arch. Pathol. Lab. Med 2004;128:1351–9. [PubMed: 15578878]
59. Shine J, Dalgarno L. The 3'-terminal sequence of *Escherichia coli* 16S ribosomal RNA: complementarity to nonsense triplets and ribosome binding sites. Proc .Natl. Acad. Sci. USA 1974;71:1342–6. [PubMed: 4598299]
60. Hui A, de Boer HA. Specialized ribosome system: preferential translation of a single mRNA species by a subpopulation of mutated ribosomes in *Escherichia coli*. Proc .Natl. Acad. Sci. USA 1987;84:4762–6. [PubMed: 2440028]
61. Hui A, Jhurani P, de Boer HA. Directing ribosomes to a single mRNA species: a method to study ribosomal RNA mutations and their effects on translation of a single messenger in *Escherichia coli*. Methods Enzymol 1987;153:432–52. [PubMed: 2828845]
62. Mullis K, Faloona F, Scharf S, Saiki R, Horn G, Erlich H. Specific enzymatic amplification of DNA *in vitro*: the polymerase chain reaction. Cold Spring Harb. Symp. Quant. Biol 1986;51:263–73. [PubMed: 3472723]
63. Mullis KB, Faloona FA. Specific synthesis of DNA *in vitro* via a polymerase-catalyzed chain reaction. Methods Enzymo 1987;155:335–50.
64. Higuchi R, Krummel B, Saiki RK. A general method of *in vitro* preparation and specific mutagenesis of DNA fragments: study of protein and DNA interactions. Nucleic Acids Res 1988;16:7351–67. [PubMed: 3045756]
65. Hanahan D. Studies on transformation of *Escherichia coli* with plasmids. J. Mol. Biol 1983;166:557–80. [PubMed: 6345791]
66. Luria SE, Burrous JW. Hybridization between *Escherichia coli* and *Shigella*. J. Bacteriology 1957;74:461–476.
67. Dower WJ, Miller JF, Ragsdale CW. High efficiency transformation of *E. coli* by high voltage electroporation. Nucleic Acids Res 1988;16:6127–45. [PubMed: 3041370]

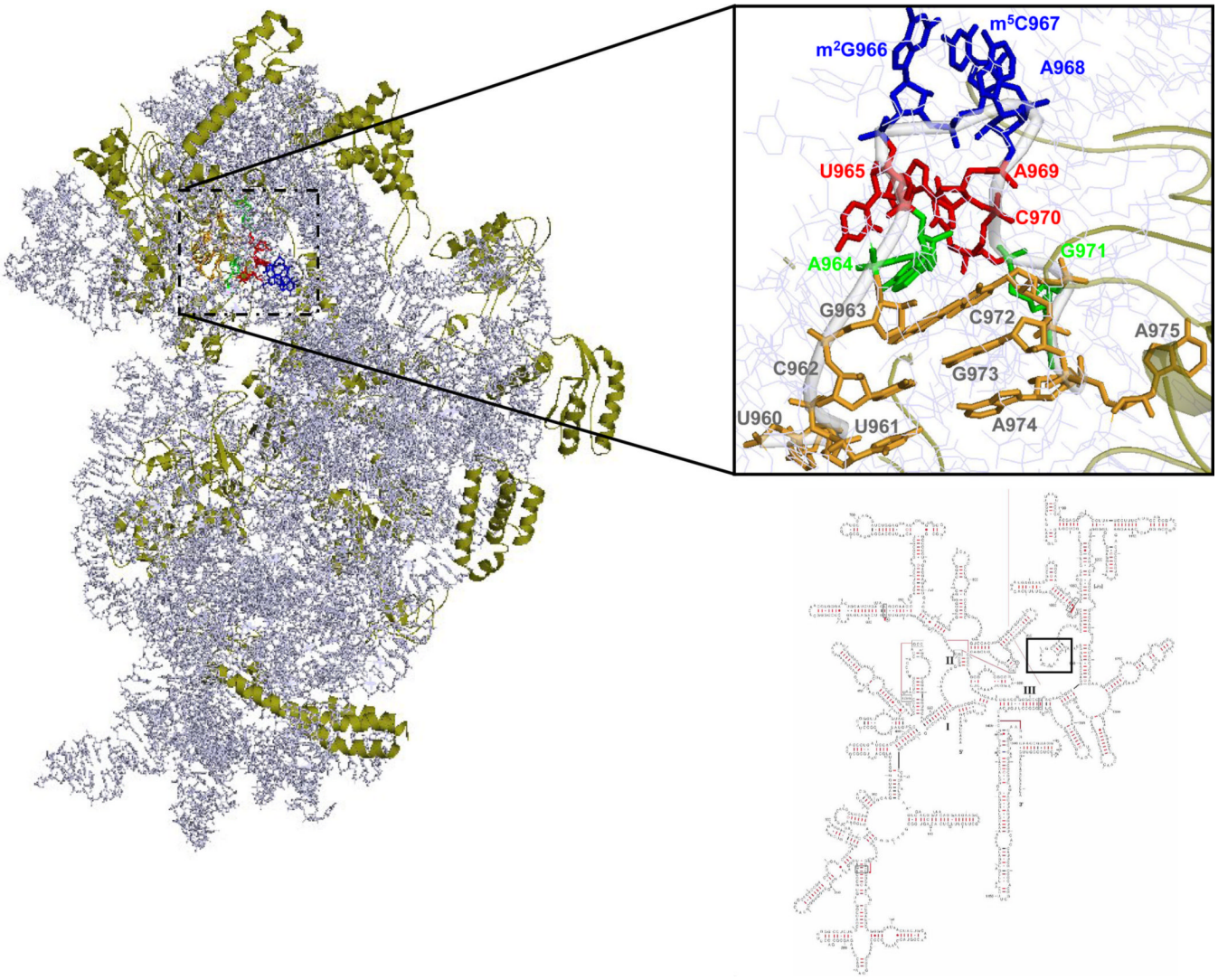

Figure 1.
Location of the 970 loop in the 16S rRNA of *E. coli*. Nucleotides in red are conserved among the three domains and organelles.

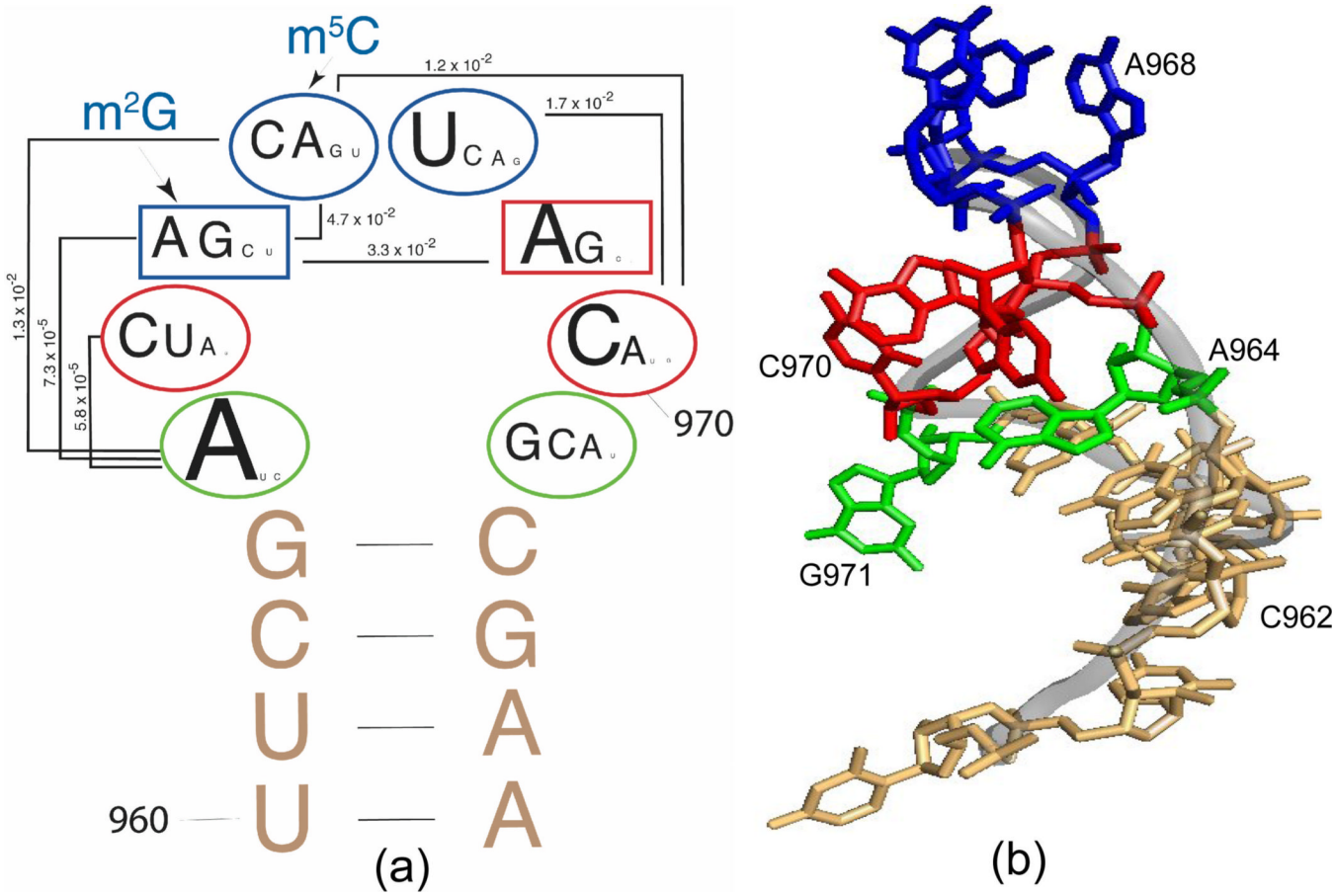

Figure 2.

Analysis of 970 loop mutants. a) Letter sizes are scaled to reflect the relative abundance of that nucleotide in the selected pool at each position. Covariation between nucleotides is indicated by solid lines. Positions where nucleotide identity significantly correlates with function (ANOVA) are boxed. The red and blue colors indicate the nucleotides involved in formation of the two stacked triples seen in the crystal structure. b) Structure of the 970 loop.[25] Stacked nucleotides are colored corresponding to the coloring in a).

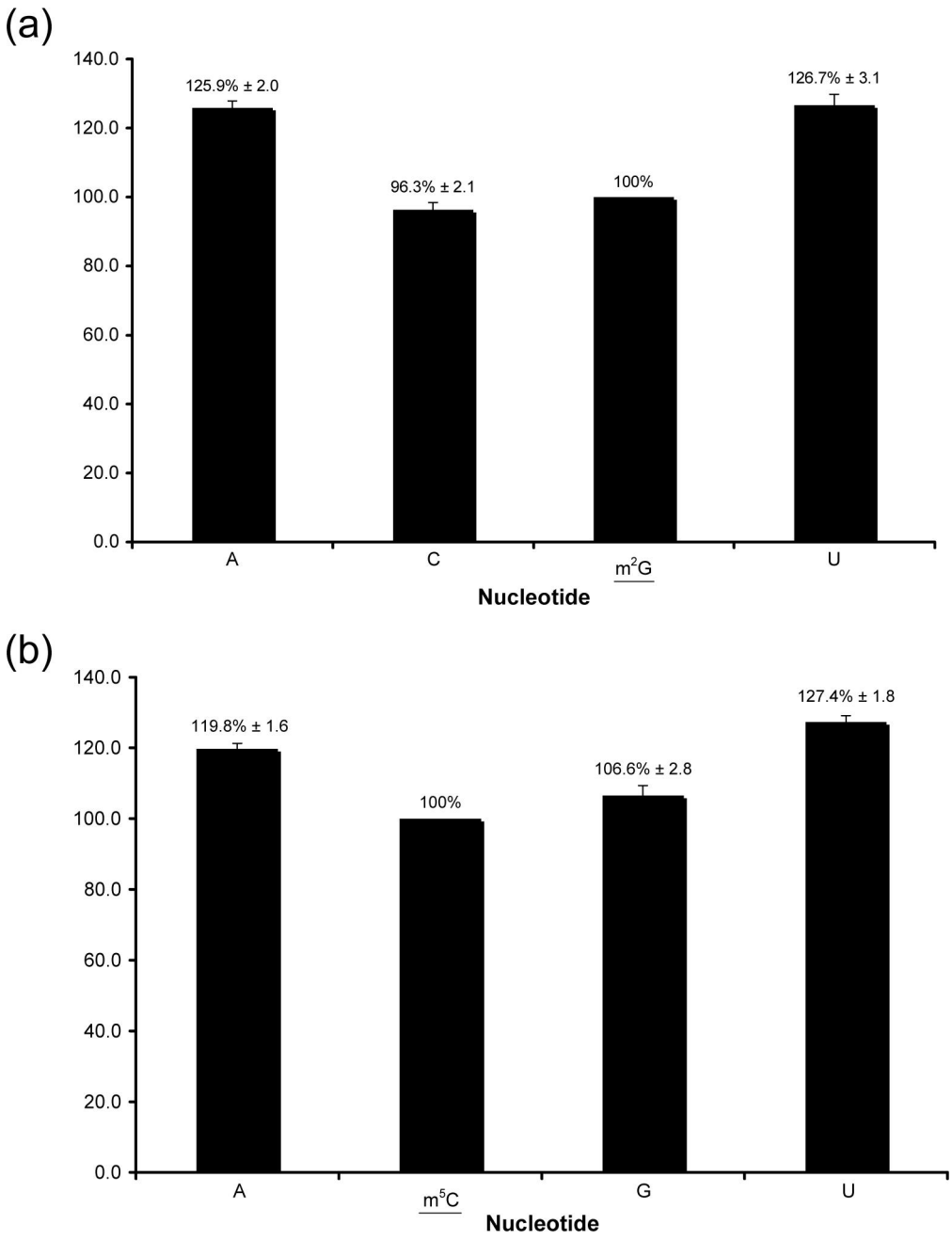

Figure 3.

m^2G966 and m^5C967 single and double mutants. a) The percent function of each single mutation at position 966 as a percent of the wild-type function. The wild-type sequence is underlined. b) The percent function of each single mutation at position 967 as a percent of the wild-type function. The wild type nucleosides are underlined.

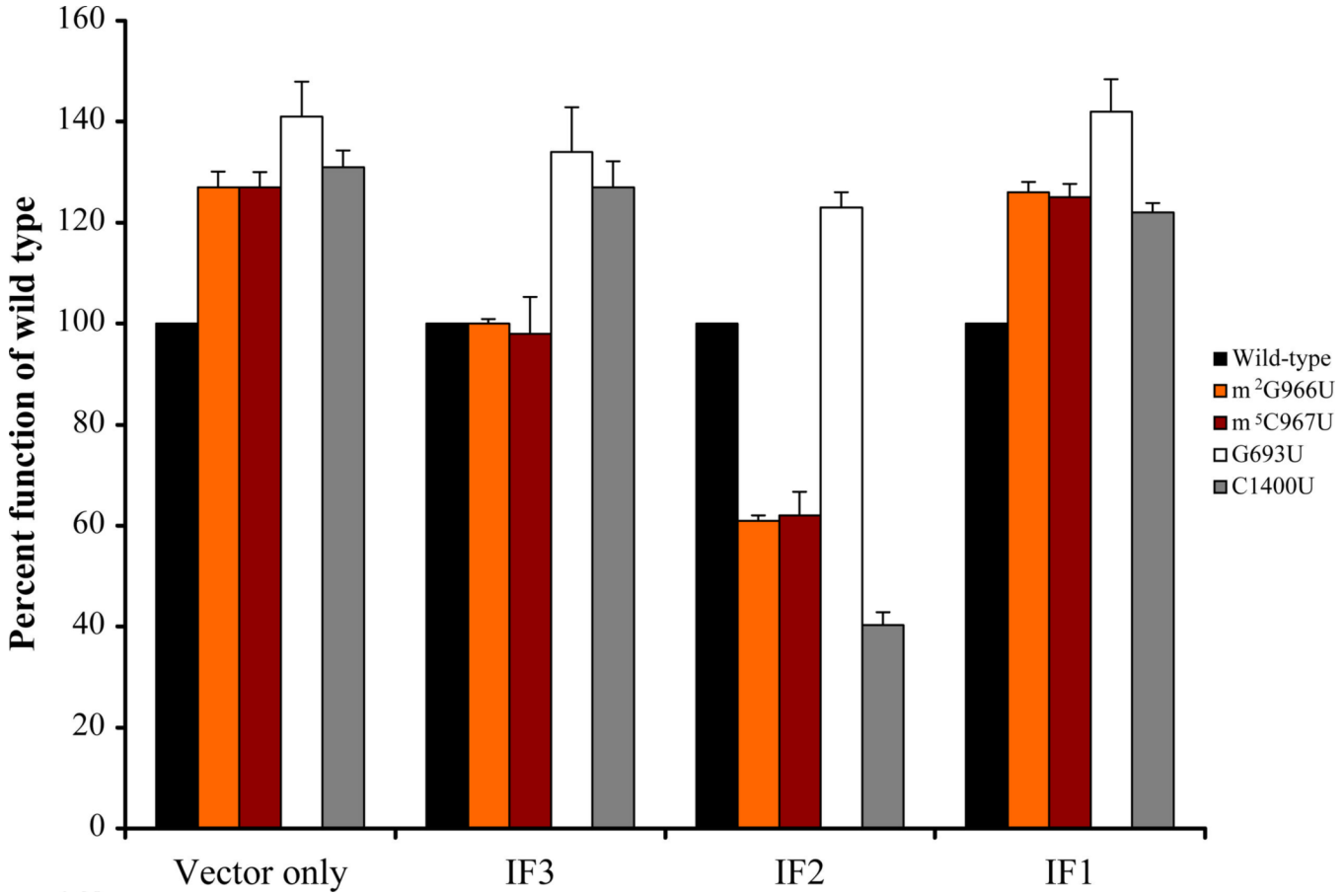

Figure 4.

Over-expression of initiation factors in the presence of m^2G966U and m^5C967U mutations. Four mutants (m^2G 966U, m^5C967U, G693U, and C1400U) that produce more GFP than wild type ribosomes were co-expressed with IF1, IF2 and IF3 and assayed. The G693U mutant was shown earlier to produce hyperactive ribosomes and was included as a control since its effect on ribosome function is unlikely to be related to the effects of mutations in the 970 loop. Data are presented as percent activity of the mutants compared to the wild-type in the presence of excess IF2. Over-expression of IF2 was inhibitory to all of the 970 mutants. Co-expression of IF1 or IF3 with wild-type ribosomes stimulated GFP production by approximately 10% compared with the vector only control. In the presence of excess IF2, however, wild-type ribosomes produced only 35% as much GFP as the vector only control (not shown).

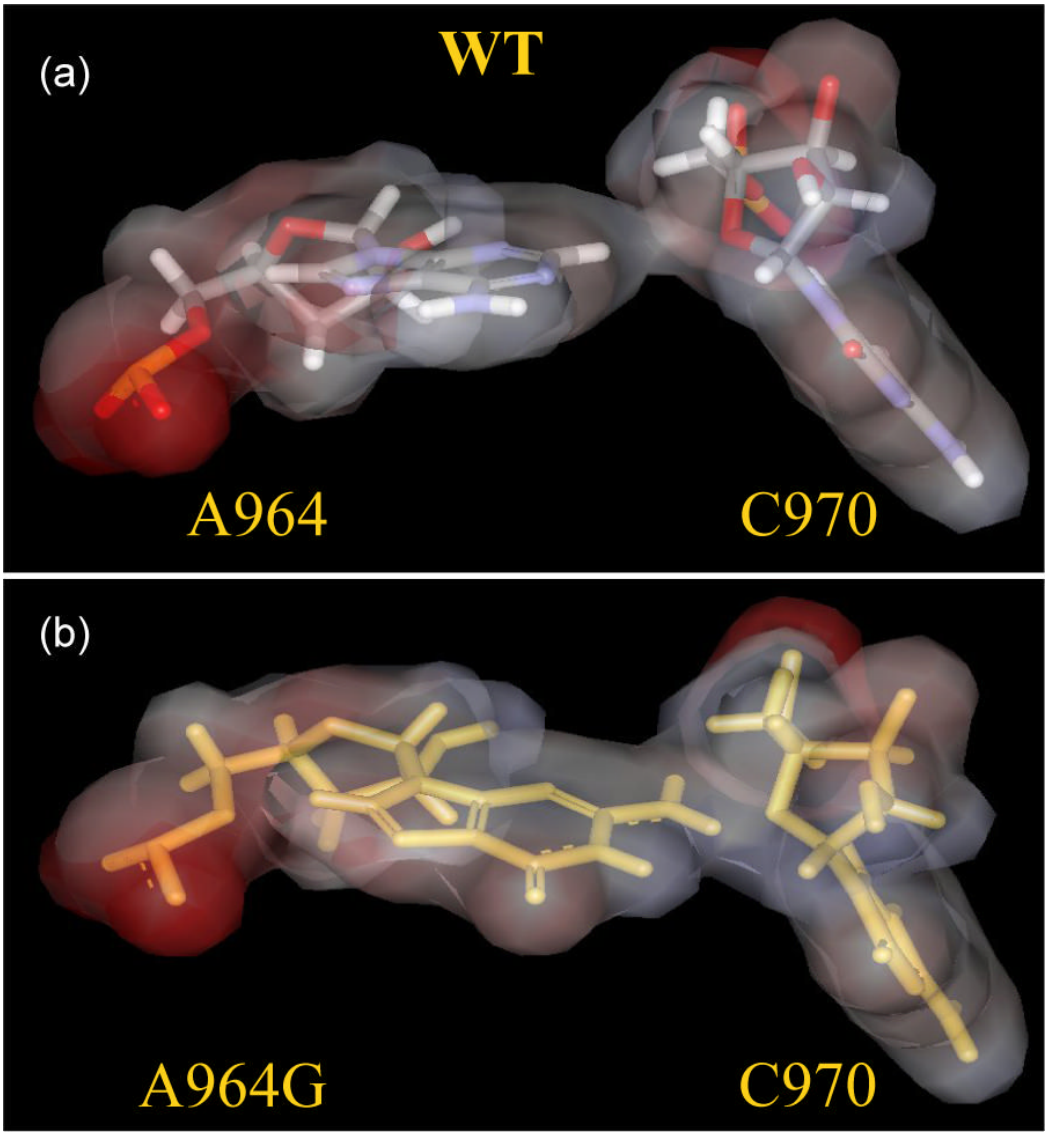

Figure 5.
Modeling of the A964G mutation. (a). Wild-type structure. (b). A964G mutation. The N2 of the A964G mutation causes steric clash with the sugar of position 970 which may disrupt the stacking interactions between positions 965, 969 and 970. Disruption of this stacking interaction may be detrimental to ribosome function.

Table 1

Sequences of functional 970 loop mutants.

Samples	Sequences[b]								Number of mutations[c]	Percent function[d]
	964	965	966	967	968	969	970	971		
WT[a]	A	U	G	C	A	A	C	G	0	100
1	A	U	G	**A**	A	A	C	G	1	119.8 (±1.6)
2	A	U	G	C	A	A	C	**U**	1	94.3 (±3.3)
3	A	**C**	G	**A**	**U**	A	C	G	3	54.3 (±2.8)
4	**U**	**C**	G	C	**U**	A	**A**	**C**	5	39.8 (±2.6)
5	A	U	G	C	**U**	A	**A**	**C**	3	39.7 (±2.0)
6	A	U	G	**A**	**U**	A	C	G	2	39.2 (±1.2)
7	A	U	G	C	**G**	**G**	C	G	2	38.1 (±1.3)
8	A	U	**C**	**A**	**C**	A	C	G	3	37.3 (±1.6)
9	A	**C**	G	**A**	A	A	C	**A**	3	35.1 (±1.7)
10	A	U	**A**	**A**	**U**	**G**	C	G	4	34.9 (±1.7)
11	A	U	G	C	**C**	A	C	**A**	2	34.4 (±2.5)
12	A	**G**	G	**G**	A	**G**	**A**	**A**	5	34.3 (±1.9)
13	A	U	G	C	**C**	A	C	**C**	2	34.3 (±1.3)
14	A	U	**C**	**G**	A	**G**	**G**	G	4	34.2 (±0.5)
15	A	**C**	G	C	**G**	A	C	G	2	33.7 (±1.0)
16	A	U	**A**	**A**	**U**	**G**	C	**C**	5	32.2 (±0.4)
17	A	**C**	G	C	**C**	**G**	C	G	3	32.0 (±1.9)
18	A	**A**	G	C	**G**	**G**	C	G	3	31.6 (±1.2)
19	A	**A**	**A**	C	**U**	A	C	G	3	31.5 (±1.3)
20	A	**C**	**A**	**A**	**U**	A	C	**C**	5	31.4 (±1.8)
21	**U**	**C**	G	**U**	**U**	A	C	**A**	5	30.7 (±0.4)
22	**U**	**C**	G	C	**U**	A	C	**C**	4	30.0 (±0.8)
23	A	**C**	G	**A**	**U**	A	C	**U**	4	29.8 (±1.6)
24	A	**C**	**A**	**A**	**U**	A	C	**C**	5	29.7 (±1.8)
25	A	**A**	G	**G**	**U**	**G**	C	G	4	29.7 (±1.3)
26	A	**A**	G	**U**	**U**	A	C	**C**	4	28.9 (±2.1)
27	A	**C**	G	**G**	**U**	A	C	**C**	4	28.7 (±3.2)
28	A	U	**A**	**A**	**U**	A	C	**A**	4	28.5 (±1.8)
29	A	**C**	**A**	**A**	**C**	A	C	G	4	28.3 (±2.6)
30	A	**C**	**A**	**A**	**U**	A	**A**	G	5	28.1 (±1.4)
31	A	**C**	**A**	**G**	**U**	A	**A**	G	5	27.6 (±1.5)
32	**U**	**A**	G	C	**U**	A	C	**A**	4	27.3 (±1.5)
33	A	**G**	**A**	**G**	**U**	A	C	G	4	27.1 (±2.1)
34	**C**	**A**	**C**	**A**	**C**	A	C	**A**	6	26.9 (±0.7)
35	A	U	**A**	**G**	**U**	A	**A**	G	4	26.8 (±1.5)
36	A	**C**	G	C	**U**	**G**	C	**C**	4	26.7 (±1.7)
37	A	**C**	**A**	C	**C**	A	C	**A**	4	26.5 (±2.4)
38	**U**	**C**	G	C	**U**	A	**A**	G	4	26.4 (±1.3)
39	A	U	G	C	**U**	A	**A**	**A**	3	26.3 (±3.1)
40	A	U	**A**	**A**	**U**	A	**A**	G	4	26.1 (±2.7)
41	A	**C**	G	**A**	**U**	**G**	**A**	G	5	26.1 (±1.3)
42	A	U	**A**	C	**C**	A	C	G	2	26.0 (±2.3)
43	A	**C**	**A**	C	**G**	A	C	G	3	25.8 (±0.8)
44	A	**A**	G	C	**U**	A	**A**	**A**	4	25.7 (±0.1)
45	A	**C**	**A**	**A**	**U**	A	C	**U**	5	25.0 (±0.8)
46	A	**C**	**A**	**A**	**U**	A	**A**	**C**	6	24.7 (±2.7)
47	A	U	G	C	**C**	**G**	C	**A**	3	24.5 (±1.3)
48	**C**	**A**	**A**	**A**	**U**	A	C	**A**	6	24.5 (±0.6)
49	A	**A**	**A**	C	**U**	A	C	**A**	4	24.5 (±2.0)
50	A	**C**	**A**	C	**U**	A	**A**	**C**	5	24.4 (±1.2)

Samples	Sequences[b]								Number of mutations[c]	Percent function[d]
	964	965	966	967	968	969	970	971		
51	A	U	**A**	**A**	**C**	A	C	**C**	4	23.8 (±2.4)
52	A	**G**	G	C	**U**	A	**A**	**C**	4	23.6 (±0.6)
53	A	**C**	**U**	C	A	A	C	G	2	23.4 (±0.1)
54	**C**	**C**	G	**U**	**U**	A	C	**A**	5	23.4 (±1.0)
55	**U**	**C**	**A**	**A**	**U**	A	**A**	**C**	7	23.1 (±1.4)
56	A	**C**	**A**	**G**	**U**	A	**A**	**C**	6	23.0 (±1.4)
57	A	**A**	**U**	C	**C**	A	C	G	3	22.6 (±0.6)
58	A	**C**	**A**	C	**U**	**G**	C	**C**	5	22.4 (±1.7)
59	A	U	**A**	**A**	**U**	A	**A**	**C**	5	22.0 (±2.6)
60	A	U	G	**G**	**C**	**G**	C	**A**	4	21.6 (±0.5)
61	A	**A**	G	C	**G**	A	**A**	**C**	4	21.6 (±2.0)
62	A	**C**	**A**	**A**	**C**	A	C	**C**	5	21.1 (±2.0)
63	A	**A**	G	C	A	**G**	**U**	G	3	20.9 (±1.4)
64	A	**C**	**A**	**A**	**U**	**G**	**A**	**C**	7	20.8 (±0.4)
65	A	U	**A**	C	**G**	A	C	G	2	20.5 (±0.4)
66	A	**C**	**A**	**A**	**C**	**C**	C	G	5	19.9 (±2.9)
67	A	U	G	**A**	**U**	**G**	**A**	**C**	5	19.7 (±2.0)
68	A	**C**	**A**	**A**	**U**	A	**A**	**A**	6	19.2 (±1.5)
69	A	**A**	G	**G**	A	**G**	**G**	**U**	5	19.2 (±1.9)
70	A	**C**	**A**	C	A	A	**A**	G	3	18.8 (±1.1)
71	A	U	**A**	C	**U**	A	**A**	**A**	4	18.3 (±1.6)
72	A	**A**	G	C	**U**	**G**	**U**	**C**	5	18.1 (±0.6)
73	A	U	**A**	**A**	**C**	A	**A**	**A**	5	18.1 (±1.1)
74	A	U	**A**	**A**	**U**	**C**	C	**C**	5	18.0 (±0.2)
75	**C**	**A**	**C**	**A**	**U**	A	C	G	5	17.7 (±2.0)
76	A	U	G	C	A	A	**G**	**A**	2	17.6 (±2.2)
77	A	**C**	**C**	C	**U**	A	C	G	3	17.5 (±1.3)
78	A	**C**	G	C	A	A	**U**	G	2	16.9 (±0.2)
79	A	U	**C**	**A**	A	**G**	C	G	3	16.2 (±1.0)
80	A	**C**	**A**	**A**	A	**G**	C	**C**	5	16.1 (±2.2)
81	A	U	**A**	**U**	**U**	**C**	C	**A**	5	15.8 (±1.2)
82	A	**C**	**A**	**A**	A	A	C	**A**	4	15.0 (±2.0)
83	A	U	**A**	**G**	**C**	A	**A**	G	4	15.0 (±2.6)
84	A	U	**A**	**U**	**C**	**G**	**A**	G	5	14.8 (±0.4)
85	A	**C**	**A**	**U**	**C**	A	**A**	**C**	6	13.9 (±1.2)
86	A	U	**A**	C	**U**	**G**	**U**	G	4	13.6 (±1.3)
87	A	**C**	**A**	**A**	A	**G**	**A**	**A**	6	13.6 (±0.8)
88	A	**C**	G	C	**U**	**G**	C	G	3	12.9 (±0.8)
89	A	U	**U**	**A**	**C**	**G**	C	G	4	12.5 (±0.1)
90	**C**	**A**	**C**	**U**	**C**	A	C	G	5	12.4 (±0.3)
91	A	**C**	**A**	**U**	**C**	A	C	**U**	5	12.3 (±0.1)
92	A	**C**	**A**	**G**	**U**	**G**	**A**	**A**	7	12.2 (±2.8)
93	A	**C**	**C**	C	**U**	**G**	C	**A**	5	11.8 (±1.4)
94	A	**A**	**A**	C	A	**G**	C	**A**	4	11.5 (±3.4)
95	A	U	**C**	**A**	**G**	**C**	**U**	**A**	6	11.4 (±2.8)
96	**C**	**A**	**C**	**A**	**C**	**G**	**A**	G	7	11.4 (±2.6)
97	A	U	**U**	C	**U**	A	C	**C**	3	11.4 (±2.0)
98	A	**C**	**U**	**A**	**U**	**U**	C	G	5	11.0 (±0.2)
99	**U**	**C**	**U**	C	**U**	A	**A**	**C**	6	10.9 (±1.0)
100	A	U	G	**A**	A	**G**	C	**C**	3	10.4 (±3.4)
101	**U**	**C**	G	**G**	**C**	**C**	**G**	**A**	7	10.2 (±3.2)
102	**C**	**A**	**C**	**U**	**U**	**G**	C	**A**	7	10.1 (±0.4)
103	A	**C**	**U**	**A**	**U**	**G**	C	**C**	6	10.0 (±2.8)
104	A	**C**	**C**	C	**U**	A	C	**C**	4	10.0 (±1.9)

Samples	Sequences[b]								Number of mutations[c]	Percent function[d]
	964	965	966	967	968	969	970	971		
105	A	U	**C**	**G**	**U**	**G**	C	G	4	9.8 (±3.0)
106	A	**C**	**C**	**U**	**U**	A	C	**C**	5	9.5 (±1.8)
107	A	**A**	**A**	**A**	**U**	**G**	**A**	**C**	7	9.5 (±1.3)

[a] Sequence and function of the unmutated construct (WT, wild type).

[b] The 970 loop sequences selected from the pool of functional mutants. Mutations are underlined.

[c] The number of mutations in each sequence.

[d] The level of function for each mutant with standard error. The function is an based on at least three independent assays.

Table 2

Nucleotide distribution of selected mutants.

Nucleotide	964	965	966	967	968	969	970	971
A. Nucleotide distribution among viable mutants [a]								
A	92 (56)	20 (12)	46 (28)	41 (24)	17 (7)	67 (50)	32 (19)	28 (15)
C	7 (3)	48 (29)	14 (3)	42 (29)	23 (13)	5 (0)	66 (44)	33 (21)
G	0	3 (3)	40 (32)	14 (9)	7 (6)	34 (15)	4 (1)	41 (26)
U	8 (6)	36 (21)	7 (2)	10 (3)	60 (39)	1 (0)	5 (1)	5 (3)
p [b]	4.8×10^{-46} (1.2×10^{-24})	2.6×10^{-9} (3.5×10^{-5})	6.3×10^{-9} (3.4×10^{-10})	3.5×10^{-7} (4.1×10^{-6})	5.9×10^{-13} (1.3×10^{-9})	1.3×10^{-22} (3.9×10^{-15})	1.3×10^{-20} (1.7×10^{-16})	6.5×10^{-6} (4.1×10^{-4})
B. Phylogenetic variation among bacteria								
A	11690	3451	140	1346	9745	11676	270	374
C	6	1507	65	10095	55	28	11450	185
G	9	389	10793	221	44	17	12	11100
U	19	6379	729	69	1886	6	3	70
Deleted	12	10	9	5	6	9	1	7

Numbers in parenthesis indicate the distribution of mutants with >20% function.

The wild-type sequence is in red and underlined.

[a] Nucleotide distribution in 107 selected mutants.

[b] Probability of random distribution based on Chi - square analysis.

Table 3

Interaction between positions 967 and 1400

Mutation[a]		Activity	
1400	967	Observed[b]	Expected[c]
C	C	100	
A	C	17.1 (±0.1)	
C	**A**	119.8 (±1.6)	
A	**A**	22.2 (±0.5)	20.5
G	C	15.5 (±0.2)	
C	**A**	119.8 (±1.6)	
G	**A**	13.3 (±0.5)	18.6
U	C	129.5 (±2.5)	
C	**A**	119.8 (±1.6)	
U	**A**	120.5 (±3.2)	155.1
A	C	17.1 (±0.1)	
C	**G**	106.6 (±2.8)	
A	**G**	17.1 (±0.4)	18.2
G	C	15.5 (±0.2)	
C	**G**	106.6 (±2.8)	
G	**G**	7.5 (±0.2)	16.5
U	C	129.5 (±2.5)	
C	**G**	106.6 (±2.8)	
U	**G**	88.7 (±3.7)	138.0
A	C	17.1 (±0.1)	
C	**U**	127.4 (±1.8)	
A	**U**	14.1 (±0.3)	21.8
G	C	15.5 (±0.2)	
C	**U**	127.4 (±1.8)	
G	**U**	6.9 (±1.6)	19.7
U	C	129.5 (±2.5)	
C	**U**	127.4 (±1.8)	
U	**U**	113.2 (±1.6)	165.0

[a] Mutations are shown in red and underlined.

[b] Mean GFP value based on three independent assays (standard error).

[c] Product of the mean activities of the single mutants.